J. Fluid Mech. (2000), *vol.* 403, *pp.* 153–172. Printed in the United Kingdom

Instability of rotating convection

By S. M. COX AND P. C. MATTHEWS

School of Mathematical Sciences, University of Nottingham, University Park, Nottingham NG7 2RD, UK

(Received 16 September 1998 and in revised form 18 August 1999)

Convection rolls in a rotating layer can become unstable to the Küppers–Lortz instability. When the horizontal boundaries are stress free and the Prandtl number is finite, this instability diverges in the limit where the perturbation rolls make a small angle with the original rolls. This divergence is resolved by taking full account of the resonant mode interactions that occur in this limit: it is necessary to include two roll modes and a large-scale mean flow in the perturbation. It is found that rolls of critical wavelength whose amplitude is of order ε are always unstable to rolls oriented at an angle of order $\varepsilon^{2/5}$. However, these rolls are unstable to perturbations at an infinitesimal angle if the Taylor number is greater than $4\pi^4$. Unlike the Küppers–Lortz instability, this new instability at infinitesimal angles does not depend on the direction of rotation; it is driven by the flow along the axes of the rolls. It is this instability that dominates in the limit of rapid rotation. Numerical simulations confirm the analytical results and indicate that the instability is subcritical, leading to an attracting heteroclinic cycle. We show that the small-angle instability grows more rapidly than the skew-varicose instability.

1. Introduction

Convection in a rotating layer of fluid has been the subject of a great deal of theoretical and experimental research. This problem is relevant to convectively driven fluid flows in the Earth's atmosphere, ocean and interior and also in the Sun and other stars, where the influence of rotation is generally important. Moreover, rotating convection generates some interesting dynamics, with a much more complicated structure than in the non-rotating case.

As first demonstrated by Küppers & Lortz (1969), convection rolls can become unstable to rolls with a different orientation. In the limit of infinite Prandtl number, Küppers & Lortz (1969) showed that, provided the Taylor number is greater than 2285, this instability occurs at onset, with the angle between the two sets of rolls being approximately 58°. It follows that the bifurcation from the stationary solution leads directly to a time-dependent flow. By considering three sets of rolls at an angle of 60°, Busse & Heikes (1980) showed that the dynamics can take the form of an attracting heteroclinic cycle, with switching between the rolls occurring in an apparently random, noise-dependent way. When non-Boussinesq effects are incorporated into the model, a subcritical bifurcation to steady hexagons occurs; this branch of solutions becomes unstable as the Rayleigh number is increased, and there is a stable limit cycle (Swift 1984; Soward 1985).

At finite Prandtl number with stress-free boundaries, there is an additional complication. As originally found by J. W. Swift and reported by Clune & Knobloch (1993), the Küppers–Lortz instability diverges as the angle between the two sets of rolls

tends to zero, for any value of the rotation rate. This means that the coefficient in the relevant amplitude equations, and hence the growth rate of the instability, tends to infinity. This suggests that rolls are always unstable to small-angle perturbations, but also indicates a breakdown in the general theory given by Clune & Knobloch (1993) in the case of stress-free boundary conditions at finite Prandtl number.

The origin of the breakdown in the analysis is a large-scale two-dimensional flow with vertical vorticity. With stress-free boundaries, this mean flow, independent of the vertical coordinate, is marginal in the sense that its decay rate tends to zero as its horizontal length scale increases. Its evolution must therefore be included in any treatment of the stability problem for rolls by means of amplitude equations. As shown by Zippelius & Siggia (1983), these mean flows also play a crucial role in the dynamics of non-rotating convection, and tend to have a destabilizing influence by coupling together two different perturbation rolls. The work of Zippelius & Siggia (1983) was, however, incomplete, and further mechanisms of instability were considered by Busse & Bolton (1984) and later by Bernoff (1994). Our work extends that of Bernoff (1994) to the rotating case.

The vanishing decay rate of the slowly varying mean flows is peculiar to stress-free boundaries. With rigid boundaries, for example, the Küppers–Lortz instability still occurs (Küppers 1970; Busse & Clever 1979*b*; Clever & Busse 1979), but there is no divergence at small angles, because the large-scale flow is strongly damped.

Since stress-free boundaries cannot be achieved in the laboratory, their relevance can be questioned. However, stress-free boundaries may be appropriate in some astrophysical applications; moreover, they are very commonly used in analytical work, since they allow simple trigonometric eigenfunctions, and also in numerical simulations.

The effect of a mean flow on the Küppers–Lortz instability has previously been considered by Ponty, Passot & Sulem (1997). They obtained an asymptotic scaling in which the angle between the rolls is of order $\varepsilon^{2/3}$ and the growth rate of the instability is of order $\varepsilon^{4/3}$, where ε is the order of magnitude of the amplitude of the original rolls. However, Ponty *et al.* (1997) included only a single set of perturbation rolls and the mean flow in their calculation. We demonstrate in this paper that such an approach is inadequate for the small-angle instability; as in the non-rotating case described by Busse & Bolton (1984) and Bernoff (1994), it is necessary to include two sets of perturbation rolls and the mean flow.

In this paper we investigate the Küppers–Lortz instability for small angles between the basic rolls and the perturbation rolls. Our work is limited to the case in which the basic rolls have exactly critical wavelength. Sections 2 and 3 summarize known results on the steady convection rolls and the Küppers–Lortz instability. The instability for small angles is studied in detail in § 4, the skew-varicose instability in § 5. The physical origin of the small-angle instability is discussed in § 6. Finally, some numerical investigations of the instability and its nonlinear evolution are presented in § 7.

2. Steady convection rolls

The dimensionless governing equations for convection in a fluid with kinematic viscosity ν and thermal diffusivity κ in a layer of depth d rotating about a vertical axis with angular velocity $\Omega\hat{\boldsymbol{z}}$ are

$$\frac{1}{\sigma}\left(\frac{\partial \boldsymbol{u}}{\partial t} + \boldsymbol{u}\cdot\nabla\boldsymbol{u}\right) + \tau\hat{\boldsymbol{z}}\times\boldsymbol{u} = -\nabla P + R\theta\hat{\boldsymbol{z}} + \nabla^2\boldsymbol{u}, \tag{2.1}$$

$$\frac{\partial \theta}{\partial t} + \boldsymbol{u} \cdot \nabla \theta - w = \nabla^2 \theta, \tag{2.2}$$

where $\boldsymbol{u} = (u, v, w)$ is the fluid velocity, θ is the temperature perturbation from the conduction state and P is the pressure. The dimensionless parameters are the Rayleigh number R, the Prandtl number $\sigma = \nu/\kappa$ and the rotation parameter $\tau = 2\Omega d^2/\nu$ which is the square root of the Taylor number.

We assume that the boundaries are stress-free and thermally conducting, so that

$$w = \frac{\partial u}{\partial z} = \frac{\partial v}{\partial z} = \theta = 0 \tag{2.3}$$

at the boundaries $z = 0$ and $z = 1$. These conditions ensure that the linear eigenfunctions are sinusoidal so that analytical solutions to the linear and weakly nonlinear stability problems can be obtained. The linear theory for this problem is well known (Chandrasekhar 1961). The stationary state is unstable to convection with a wavenumber k if the Rayleigh number exceeds the critical value

$$R_m = \frac{(\pi^2 + k^2)^3 + \tau^2 \pi^2}{k^2}. \tag{2.4}$$

The marginal curve $R = R_m(k)$ has a minimum at $k = k_c$, where $R = R_c = 3(\pi^2 + k_c^2)^2$. The value of k_c, which corresponds to the first mode to become unstable as R is increased, may be found from

$$\tau^2 \pi^2 = (2k_c^2 - \pi^2)(\pi^2 + k_c^2)^2, \tag{2.5}$$

an identity that is used repeatedly in our analysis. It is easily seen from (2.5) that as the rotation rate is increased, the preferred wavenumber increases and the convection cells correspondingly become increasingly narrow. In this paper we consider the stability of rolls with the critical wavenumber: therefore wherever k appears subsequently, k_c is intended. Perturbations to the rolls need not have critical wavenumber.

The weakly nonlinear theory is well established (see, e.g., Bassom & Zhang 1994). The variables $\boldsymbol{u}$ and θ are expanded in a small parameter ε as

$$\boldsymbol{u} \sim \varepsilon \boldsymbol{u}_1 + \varepsilon^2 \boldsymbol{u}_2 + \varepsilon^3 \boldsymbol{u}_3 + \cdots, \tag{2.6}$$

$$\theta \sim \varepsilon \theta_1 + \varepsilon^2 \theta_2 + \varepsilon^3 \theta_3 + \cdots, \tag{2.7}$$

with $R = R_c + \varepsilon^2 R_2$. At first order in ε the linear problem is obtained. After eliminating P by taking $\hat{\boldsymbol{z}} \cdot \nabla \times$ and $\hat{\boldsymbol{z}} \cdot \nabla \times \nabla \times$ of (2.1), the solution for convection rolls with their axes aligned in the y-direction is found to be

$$w_1 = A \sin \pi z \sin kx, \tag{2.8}$$

$$u_1 = A \cos \pi z \cos kx \, \pi/k, \tag{2.9}$$

$$v_1 = -A \cos \pi z \cos kx \, \tau\pi/ka^2, \tag{2.10}$$

$$\theta_1 = A \sin \pi z \sin kx \, /a^2, \tag{2.11}$$

where the amplitude A is arbitrary at this stage and we have introduced $a^2 = \pi^2 + k^2$. At second order the solution is

$$w_2 = u_2 = 0, \tag{2.12}$$

$$v_2 = -A^2 \pi^2 \tau \sin 2kx \, /8k^3 \sigma a^2, \tag{2.13}$$

$$\theta_2 = -A^2 \sin 2\pi z \, /8\pi a^2. \tag{2.14}$$

At third order in ε a solvability condition is obtained, yielding the following relationship between R_2 and A:

$$8k^4\sigma^2a^2R_2 = (\sigma^2k^4R_c - \tau^2\pi^4)A^2. \tag{2.15}$$

It follows that the bifurcation to rolls is supercritical provided $\sigma > \sigma_c(\tau) = (\tau^2\pi^4/k^4R_c)^{1/2}$. The function $\sigma_c(\tau) \to 0$ in the limits of small and large τ; its maximum value, $\sigma_c = 1/3$, occurs when $\tau = 2\pi^2$. We assume throughout that $\sigma > \sigma_c$.

3. The Küppers–Lortz instability

The original analysis of Küppers & Lortz (1969) assumed infinite Prandtl number and showed that the weakly nonlinear convection rolls are unstable if $\tau^2 > 2285$. The instability takes the form of convection rolls aligned at some angle Φ to the original rolls, so that, for example, the vertical velocity takes the form

$$w \sim \varepsilon A \sin\pi z \sin kx + \delta B \sin\pi z \sin(kx + mx + ly), \tag{3.1}$$

where $\tan\Phi = l(k+m)^{-1}$ and $\delta \ll \varepsilon$ is the amplitude of the perturbation. Since the calculation is weakly nonlinear, the perturbations must have wavenumbers close to the marginal circle if they are to grow. In fact, unless Φ is small, the growth rate of perturbations is captured accurately by taking the perturbation rolls to have exactly the critical wavenumber. The perturbation wavenumbers are therefore related by

$$2km + m^2 + l^2 = 0. \tag{3.2}$$

The more complicated case of finite Prandtl number is described in detail by Ponty *et al.* (1997). At order $\varepsilon\delta$, terms with a trigonometric dependence $\cos(mx + ly)$ and $\cos(2kx + mx + ly)$ are generated. At order $\varepsilon^2\delta$, a solvability condition is obtained that gives the eigenvalue corresponding to the growth rate of the perturbation. This cumbersome expression is not given here. However, we note the important feature that in the limit $l \to 0$, with ε fixed, the growth rate λ of the instability diverges (Ponty *et al.* 1997):

$$\lambda \sim \frac{\tau\pi^2\varepsilon^2A^2}{4lk\sigma a^2}. \tag{3.3}$$

Clearly, this divergence is not physical, but results from a breakdown in the asymptotic scalings used. The aim of the next section is to determine the nature of this breakdown and to obtain a correct expression for the growth rate of the instability when l becomes small.

4. The small-angle instability

In this section we consider the Küppers–Lortz instability where the perturbing B rolls make a small angle with the original A rolls. In keeping with the previous work of Küppers & Lortz (1969) and Ponty *et al.* (1997), we consider only the case where the A rolls have wavenumber k_c. The wavenumber of the perturbing B rolls is close to, but not necessarily equal to, k_c. In addition to the small-angle instability that is the focus of this paper, our scalings permit consideration of the skew-varicose instability described by Busse & Bolton (1984) and Bernoff (1994), to which the A rolls may also be susceptible; see § 5.

It is important first to consider the mode interactions involved. In the analysis summarized in § 3, neither of the secondary modes generated at $O(\varepsilon\delta)$ has a wavenumber

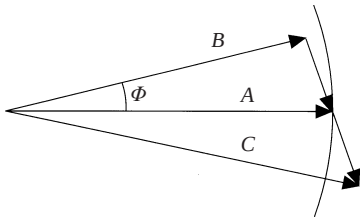

FIGURE 1. Mode interactions involved in the small-angle instability. Each arrow represents the wavevector of one of the modes involved. The marginal circle is also shown, on which the wavenumber is k_c. The basic rolls A are perturbed by the rolls B. For small angles Φ, a small-wavenumber mode is forced, which in turn forces a near-marginal mode C.

near k_c, so both of these modes are regarded as 'slaved'.† When m and l are small, however, the mode with a horizontal dependence $\cos(mx+ly)$ represents a large-scale mean flow, independent of z and varying only slowly in the horizontal. With stress-free boundaries, this mode is only weakly damped, with a decay rate $\sigma(l^2+m^2)$. If l and ε have similar orders of magnitude, this mode is no longer slaved and must be allowed to evolve independently. Furthermore, the interaction of this mean flow mode and the A rolls generates an additional mode, C, with a horizontal dependence $\sin(kx-mx-ly)$. This mode lies close to the circle of critical modes (figure 1), so it must also be included in the calculation. Since we are concerned only with the linear instability of the A rolls, it is clear that no other near-marginal modes are generated.

There are therefore three near-marginal modes involved in the instability. As found by Bernoff (1994), stability problems of the type described here are quite subtle, in the sense that apparently small terms can significantly affect the growth rates of perturbations. Bernoff's approach involves deriving a set of equations for the amplitudes of the rolls and the mean flow. In contrast to the usual Newell–Whitehead–Segel equations (Newell & Whitehead 1969; Segel 1969), these amplitude equations contain terms of mixed asymptotic order; without this feature, they cannot reproduce the established long-wavelength stability boundaries of convection rolls (Busse & Bolton 1984). Thus, although they have no strict mathematical justification, these mixed-order amplitude equations prove effective.

We adopt a similar approach in tackling the corresponding stability problem for rotating convection. Thus we begin by deriving amplitude equations of mixed asymptotic order by systematic, if not rigorous, means. These equations extend those of Bernoff (1994), and collapse to his when $\tau = 0$ (with the exception of one term, which Bernoff omitted, but which, fortunately, plays no part in the instabilities discussed here). Consideration of the stability of convection rolls according to these equations motivates various asymptotic balances, which we then examine. Once each balance is determined, it can be investigated systematically by an appropriate asymptotic expansion without recourse to mixed-order amplitude equations. Although we have carried out such an expansion in each case, we do not present the details because the results are no different from those based on the amplitude equations. Thus the mixed-order amplitude equations serve as a convenient organizing centre for the various scalings, but they are not essential to our arguments. The reason

† Of course, if Φ is close to 60°, the interaction between the basic and the perturbing rolls produces a mode that *is* nearly marginal. However, with our focus on the small-angle instability, we do not consider this circumstance further.

for introducing them is that otherwise it is difficult to justify the apparently obscure scalings used.

As in § 2, we expand $\boldsymbol{u}$ and θ in powers of ε according to (2.6) and (2.7), where again $R = R_c + \varepsilon^2 R_2$. Now, however, we allow the amplitude of the rolls to vary slowly on the spatial scales

$$X = \varepsilon x, \qquad Y = \varepsilon y. \tag{4.1}$$

This scaling is somewhat arbitrary, because we use our amplitude equations to infer the behaviour of the convection on a variety of different slow spatial and temporal scales. However, the choice (4.1) is particularly convenient, ensuring that all necessary terms (except one) are present in the amplitude equations. The missing term can in any event be inferred from the rotational invariance of the problem. Then (2.8)–(2.11) become

$$w_1 = \mathrm{Re}\,(-\mathrm{i}A(X, Y, t)\exp \mathrm{i}kx)\sin \pi z, \tag{4.2}$$

$$u_1 = \mathrm{Re}\,(A(X, Y, t)\exp \mathrm{i}kx\,\pi/k)\cos \pi z, \tag{4.3}$$

$$v_1 = \mathrm{Re}\,(-A(X, Y, t)\exp \mathrm{i}kx\,\tau\pi/ka^2)\cos \pi z, \tag{4.4}$$

$$\theta_1 = \mathrm{Re}\,(-\mathrm{i}A(X, Y, t)\exp \mathrm{i}kx\,/a^2)\sin \pi z, \tag{4.5}$$

where the amplitude A is now a complex function of X, Y and t.

The large-scale mean flow does not arise at this order in the expansion since it is generated by a quadratic self-interaction of the rolls. The question is then: at what order should the mean flow be introduced into the expansion? Regardless of the choice that is made, the amplitude equations contain terms of mixed asymptotic order (see, e.g., the equations of Bernoff 1994 and the analogous equations derived by Barthelet & Charru 1998 and Charru & Barthelet 1999 for interfacial waves). Ultimately, however, the point is moot because we merely use the amplitude equations to suggest other asymptotic scalings, then carry out calculations with these (consistent) scalings.

In order to compute all the terms required by our subsequent analysis, we suppose that the evolution of A with time may be written in the form

$$\frac{\partial A}{\partial t} = \varepsilon^2 \hat{A}_2 + \varepsilon^3 \hat{A}_3. \tag{4.6}$$

Then $\hat{A}_2$ and $\hat{A}_3$ are determined by applying solvability conditions at $O(\varepsilon^3)$ and $O(\varepsilon^4)$, respectively.

At $O(\varepsilon^2)$, as at all orders in ε, the solution for $\boldsymbol{u}$ and θ may be determined up to the addition of an arbitrary multiple of the linear eigensolution. Different choices of this multiple correspond to a small renormalization of A. This does not affect the leading-order terms in the amplitude equations, but it does affect higher-order terms, such as we calculate here. In order to determine $\hat{A}_3$ uniquely, therefore, it is necessary to specify a normalization condition to fix A; we apply the condition

$$\varepsilon A = \frac{2\mathrm{i}\,k}{\pi}\int_0^{2\pi/k}\int_0^1 w\,\mathrm{e}^{-\mathrm{i}kx}\sin \pi z\,\mathrm{d}z\,\mathrm{d}x. \tag{4.7}$$

Other authors, for example Cross *et al.* (1983) and Bernoff (1994), apply other normalization conditions, and so they obtain different, but equivalent, results beyond leading order in their amplitude equations.

At $O(\varepsilon^2)$, we find

$$w_2 = 0, \tag{4.8}$$

$$u_2 = \mathrm{Re}\left(\left(\frac{\mathrm{i}\pi A_X}{k^2} - \frac{\mathrm{i}\tau\pi A_Y}{k^2 a^2}\right)\exp \mathrm{i}kx\right)\cos\pi z + U(X, Y, t), \tag{4.9}$$

$$v_2 = \mathrm{Re}\left(\left(-\frac{\mathrm{i}\pi A_Y}{k^2} - \frac{\mathrm{i}\tau\pi(3k^2+\pi^2)A_X}{k^2 a^4}\right)\exp \mathrm{i}kx\right)\cos\pi z + \mathrm{Re}\left(\frac{\mathrm{i}\tau\pi^2 A^2}{8k^3\sigma a^2}\exp 2\mathrm{i}kx\right) + V(X, Y, t), \tag{4.10}$$

$$\theta_2 = \mathrm{Re}\left(\frac{2kA_X}{a^4}\exp \mathrm{i}kx\right)\sin\pi z - \frac{|A|^2}{8\pi a^2}\sin 2\pi z. \tag{4.11}$$

We have introduced a large-scale mean flow (U, V) at this order so that it advects the pattern in the leading-order contribution $\hat{A}_2$.

At $O(\varepsilon^3)$ we find $\hat{A}_2$ from applying the usual solvability condition to terms proportional to $\exp \pm \mathrm{i}kx$ and $\sin\pi z$ or $\cos\pi z$ to eliminate secular terms. We find

$$\hat{A}_2 = -\mathrm{i}kUA + \frac{k^2\gamma R_2}{12a^2}A + k^2\gamma A_{XX} - \frac{(\sigma^2 k^4 R_c - \tau^2\pi^4)\gamma}{96k^2\sigma^2 a^4}A|A|^2, \tag{4.12}$$

where

$$\gamma = \frac{12\sigma}{3k^2\sigma - k^2 + 2\pi^2}.$$

Apart from the advection term $-\mathrm{i}kUA$, these terms are those of the Newell–Whitehead–Segel equation (Newell & Whitehead 1969; Segel 1969).

Since it is necessary to consider the equations at $O(\varepsilon^4)$ in order to determine $\hat{A}_3$, we must compute the solution at $O(\varepsilon^3)$, though this is a rather tedious calculation, even using the computer algebra package Maple, as we have done. The solution is of sufficient complexity that little insight would be gained by displaying it here. Of particular significance, however, is the vertical vorticity, which at this order contains a component $\omega(X, Y, t)$, independent of depth, related to the mean flow (U, V) by

$$\left(\frac{\partial^2}{\partial X^2} + \frac{\partial^2}{\partial Y^2}\right)U = -\frac{\partial\omega}{\partial Y}, \quad \left(\frac{\partial^2}{\partial X^2} + \frac{\partial^2}{\partial Y^2}\right)V = \frac{\partial\omega}{\partial X}.$$

Indeed, we define $\varepsilon^3\omega(X, Y, t)$ to be the x- and z-average of the vertical component of the vorticity. Note that although A is in general complex, ω is real.

At $O(\varepsilon^4)$, the solvability condition to eliminate secular terms provides $\hat{A}_3$, and so (4.6) becomes

$$\begin{aligned}\frac{\partial A}{\partial t} = {} & \varepsilon^2\left\{-\mathrm{i}kUA + \frac{k^2\gamma R_2}{12a^2}A + k^2\gamma\left(\frac{\partial}{\partial X} - \frac{\varepsilon\mathrm{i}}{2k}\frac{\partial^2}{\partial Y^2}\right)^2 A - \frac{(\sigma^2 k^4 R_c - \tau^2\pi^4)\gamma}{96k^2\sigma^2 a^4}A|A|^2\right\} \\ & + \varepsilon^3\left\{-U\frac{\partial A}{\partial X} - V\frac{\partial A}{\partial Y} - \frac{2k\sigma(3k^4\sigma + 2\pi^4 - 5k^4)R_2\,\mathrm{i}}{c^2 a^4}\frac{\partial A}{\partial X}\right. \\ & + \frac{4\mathrm{i}\sigma k(-6\pi^4 - \pi^2 k^2 + 29k^4 + 9\pi^2 k^2\sigma - 15k^4\sigma)}{c^2 a^2}\frac{\partial^3 A}{\partial X^3} + \frac{\tau\pi^2}{ca^2}\left(3\frac{\partial U}{\partial Y} - \frac{\partial V}{\partial X}\right)A \\ & \left. - \frac{2(\pi^4 + 2\pi^2 k^2 - 2k^4 + 3k^4\sigma)}{ca^2}A\frac{\partial U}{\partial X}\right.\end{aligned}$$

$$-\frac{\mathrm{i}(6\pi^4-7\pi^2k^2-3\pi^2k^2\sigma+3k^4\sigma^2)\tau}{16\sigma ca^2k^3}A\frac{\partial|A|^2}{\partial Y}$$
$$+\mathrm{i}c_+\left(A^2\frac{\partial A^*}{\partial X}+|A|^2\frac{\partial A}{\partial X}\right)+\mathrm{i}c_-\left(A^2\frac{\partial A^*}{\partial X}-|A|^2\frac{\partial A}{\partial X}\right)\Bigg\}, \tag{4.13}$$

where

$$c=3k^2\sigma-k^2+2\pi^2=12\sigma/\gamma,$$

$$c_+=[9\sigma^3(\pi^2+7k^2)k^6+3\sigma^2(14\pi^4+\pi^2k^2-31k^4)k^4$$
$$+4(2k^2-\pi^2)\pi^2(3\sigma\pi^2k^2-\pi^4+2\pi^2k^2+6k^4)]/(16\sigma ca^2k^3),$$

$$c_-=\frac{(2k^2-\pi^2)(3k^4\sigma^2-3\pi^2k^2\sigma-\pi^2a^2)}{4\sigma ck^3}.$$

In writing (4.13), we have completed the linear spatial derivative term in the form $(\partial/\partial X-\frac{1}{2}\varepsilon\mathrm{i}\partial^2/\partial Y^2/k)^2A$, which reflects the rotational invariance of the original convection problem about a vertical axis – see Newell & Whitehead (1969). The extra term, proportional to $\partial^4A/\partial Y^4$, is needed in some of the scalings that follow.

An evolution equation for ω may be found by writing

$$\frac{\partial\omega}{\partial t}=\varepsilon\hat{\omega}_1+\varepsilon^2\hat{\omega}_2, \tag{4.14}$$

then averaging the vertical vorticity equation in x and z to obtain

$$\frac{\partial\omega}{\partial t}=\frac{\varepsilon}{2k^2a^2}\left\{(\pi^4-k^4)\frac{\partial^2|A|^2}{\partial X\partial Y}+\frac{\pi^2\tau}{2}\left(\frac{\partial^2|A|^2}{\partial X^2}-\frac{\partial^2|A|^2}{\partial Y^2}\right)\right\}$$
$$+\varepsilon^2\sigma\left(\frac{\partial^2\omega}{\partial X^2}+\frac{\partial^2\omega}{\partial Y^2}\right)+\frac{\varepsilon^2\mathrm{i}}{4k^3a^2}$$
$$\times\left\{\left[(\pi^4-k^4)\frac{\partial}{\partial Y}\left(A\left(\frac{\partial^2A^*}{\partial Y^2}-3\frac{\partial^2A^*}{\partial X^2}\right)\right)\right.\right.$$
$$\left.+2(\pi^4-k^4)\frac{\partial}{\partial X}\left(\frac{\partial A}{\partial Y}\frac{\partial A^*}{\partial X}\right)+2(2k^2-\pi^2)k^2\frac{\partial}{\partial Y}\left(A\frac{\partial^2A^*}{\partial X^2}\right)\right]-\mathrm{c.c.}\Bigg\}$$
$$-\frac{\mathrm{i}\pi^2\tau\varepsilon^2}{4a^4k^3}\left\{\left[(2k^2+\pi^2)\frac{\partial}{\partial X}\left(A\frac{\partial^2A^*}{\partial X^2}\right)-2(2k^2+\pi^2)\frac{\partial}{\partial Y}\left(A\frac{\partial^2A^*}{\partial X\partial Y}\right)\right.\right.$$
$$\left.\left.-\pi^2\frac{\partial}{\partial X}\left(A\frac{\partial^2A^*}{\partial Y^2}\right)\right]-\mathrm{c.c.}\right\}. \tag{4.15}$$

It is simpler to deal with the equations (4.13) and (4.15) in the form

$$\frac{\partial A}{\partial t}=\varepsilon^2\left\{-\mathrm{i}kUA+\alpha_1A+\alpha_2\left(\frac{\partial}{\partial X}-\frac{\varepsilon\mathrm{i}}{2k}\frac{\partial^2}{\partial Y^2}\right)^2A-\alpha_3A|A|^2\right\}$$
$$+\varepsilon^3\left\{-U\frac{\partial A}{\partial X}-V\frac{\partial A}{\partial Y}+\mathrm{i}\alpha_4\frac{\partial A}{\partial X}+\mathrm{i}\alpha_5\frac{\partial^3A}{\partial X^3}+\alpha_6\left(3\frac{\partial U}{\partial Y}-\frac{\partial V}{\partial X}\right)A\right.$$
$$\left.+\alpha_7A\frac{\partial U}{\partial X}+\mathrm{i}\alpha_8A\frac{\partial|A|^2}{\partial Y}+\mathrm{i}\alpha_9A\frac{\partial|A|^2}{\partial X}+\mathrm{i}\alpha_{10}\left(A^2\frac{\partial A^*}{\partial X}-|A|^2\frac{\partial A}{\partial X}\right)\right\}, \tag{4.16}$$

$$\frac{\partial\omega}{\partial t} = \varepsilon\left\{\beta_1\frac{\partial^2|A|^2}{\partial X\partial Y} + \beta_2\left(\frac{\partial^2|A|^2}{\partial X^2} - \frac{\partial^2|A|^2}{\partial Y^2}\right)\right\} + \varepsilon^2\sigma\left(\frac{\partial^2\omega}{\partial X^2} + \frac{\partial^2\omega}{\partial Y^2}\right)$$
$$+\varepsilon^2\mathrm{i}\left\{\left[\beta_3\frac{\partial}{\partial Y}\left(A\left(\frac{\partial^2 A^*}{\partial Y^2} - 3\frac{\partial^2 A^*}{\partial X^2}\right)\right)\right.\right.$$
$$\left.\left. + \ +2\beta_3\frac{\partial}{\partial X}\left(\frac{\partial A}{\partial Y}\frac{\partial A^*}{\partial X}\right) + \beta_4\frac{\partial}{\partial Y}\left(A\frac{\partial^2 A^*}{\partial X^2}\right)\right] - \text{c.c.}\right\}$$
$$+\varepsilon^2\mathrm{i}\left\{\left[\beta_5\frac{\partial}{\partial X}\left(A\frac{\partial^2 A^*}{\partial X^2}\right) - 2\beta_5\frac{\partial}{\partial Y}\left(A\frac{\partial^2 A^*}{\partial X\partial Y}\right)\right.\right.$$
$$\left.\left. + \ +\beta_6\frac{\partial}{\partial X}\left(A\frac{\partial^2 A^*}{\partial Y^2}\right)\right] - \text{c.c.}\right\}, \tag{4.17}$$

where α_1–α_{10} and β_1–β_6 are defined by comparing (4.13) and (4.15) with (4.16) and (4.17).

In the non-rotating limit, the equations (4.16)–(4.17) are equivalent to those derived by Bernoff (1994) (with the exception of the term $\mathrm{i}A_{XXX}$, which Bernoff omitted). However, our normalization condition (4.7) differs from Bernoff's and so a near-identity transformation of A and ω is necessary to bring his and our equations into agreement (after appropriately rescaling).

4.1. *Stability of rolls*

In this subsection we use (4.16) and (4.17) to investigate the stability of rolls with critical wavenumber to small-angle disturbances. To this end we write

$$A = A_0 + B(t)\exp\mathrm{i}(mx + ly) + C^*(t)\exp -\mathrm{i}(mx + ly),$$

where the unperturbed roll amplitude $A = A_0$ satisfies (2.15) and with no loss of generality is real. The perturbation amplitudes satisfy $B \ll A$ and $C \ll A$.

According to our scaling (4.1), the wavenumbers l and m should be $O(\varepsilon)$. However, as we explain below, other asymptotic scalings of l and m are necessary to reveal the stability properties of the A rolls. We therefore treat ε, l and m as independent parameters, until their relative magnitudes are decided in §§ 4.4, 4.5 and 4.6. The corresponding mean flow is driven by the vertical vorticity in the form

$$\omega = \omega(t)\exp\mathrm{i}(mx + ly) + \omega^*(t)\exp -\mathrm{i}(mx + ly).$$

Substitution of these expressions into (4.16) and (4.17), and linearization in perturbation amplitudes leads to the following system of equations for the evolution of $B(t)$, $C(t)$ and $\omega(t)$:

$$\begin{pmatrix}\dot B\\ \dot C\\ \dot\omega\end{pmatrix} = \begin{pmatrix}\Xi_{11} & \Xi_{12} & \Xi_{13}\\ \Xi_{21} & \Xi_{22} & \Xi_{23}\\ \Xi_{31} & \Xi_{32} & \Xi_{33}\end{pmatrix}\begin{pmatrix}B\\ C\\ \omega\end{pmatrix}, \tag{4.18}$$

where the coefficients of the matrix are

$$\Xi_{11} = -\alpha_2(m + \tfrac{1}{2}l^2/k)^2 - \varepsilon^2\alpha_3A_0^2 - \varepsilon^2\alpha_4 m + \alpha_5 m^3 - \varepsilon^2 l\alpha_8A_0^2 - \varepsilon^2 m\alpha_9A_0^2 + \varepsilon^2 m\alpha_{10}A_0^2,$$
$$\Xi_{12} = -\varepsilon^2\alpha_3A_0^2 - \varepsilon^2 l\alpha_8A_0^2 - \varepsilon^2 m\alpha_9A_0^2 - \varepsilon^2 m\alpha_{10}A_0^2,$$
$$\Xi_{13} = \frac{\varepsilon^3 kA_0 l}{m^2 + l^2} - \frac{\varepsilon^3\alpha_6(m^2 + 3l^2)A_0}{m^2 + l^2} - \frac{\varepsilon^3\alpha_7 lmA_0}{m^2 + l^2},$$
$$\Xi_{21} = -\varepsilon^2\alpha_3A_0^2 + \varepsilon^2 l\alpha_8A_0^2 + \varepsilon^2 m\alpha_9A_0^2 + \varepsilon^2 m\alpha_{10}A_0^2,$$
$$\Xi_{22} = -\alpha_2(-m + \tfrac{1}{2}l^2/k)^2 - \varepsilon^2\alpha_3A_0^2 + \varepsilon^2\alpha_4 m - \alpha_5 m^3 + \varepsilon^2 l\alpha_8A_0^2 + \varepsilon^2 m\alpha_9A_0^2 - \varepsilon^2 m\alpha_{10}A_0^2,$$

$$\Xi_{23} = -\frac{\varepsilon^3 k A_0 l}{m^2+l^2} - \frac{\varepsilon^3 \alpha_6 (m^2+3l^2) A_0}{m^2+l^2} - \frac{\varepsilon^3 \alpha_7 l m A_0}{m^2+l^2},$$

$$\Xi_{31} = \varepsilon^{-1}[-lm\beta_1 + (l^2-m^2)\beta_2]A_0 + \varepsilon^{-1}[\beta_3 l(3m^2-l^2) - \beta_4 m^2 l - \beta_5 m^3 + 2\beta_5 m l^2 - \beta_6 m l^2]A_0,$$

$$\Xi_{32} = \varepsilon^{-1}[-lm\beta_1 + (l^2-m^2)\beta_2]A_0 - \varepsilon^{-1}[\beta_3 l(3m^2-l^2) - \beta_4 m^2 l - \beta_5 m^3 + 2\beta_5 m l^2 - \beta_6 m l^2]A_0,$$

$$\Xi_{33} = -\sigma(m^2+l^2).$$

We seek solutions for which B, C and ω are proportional to $\exp \lambda t$, and calculate the growth rate λ for particular distinguished scalings between the small parameters ε, l and m.

As it stands, (4.18) contains terms of mixed asymptotic orders, and is therefore of uncertain value; in §§ 4.4, 4.5 and 4.6 we show how three *consistent* asymptotic scalings may be deduced from (4.18). Indeed, once these scalings are noted, the corresponding results may be obtained directly from the governing equations, without recourse to (4.18). However, in view of the rather obscure nature of two of the three crucial scalings, we find (4.18) a useful intermediate step. No one consistent asymptotic scaling can be found to cover all the necessary cases.

4.2. *Matching with the Küppers–Lortz instability*

We start our analysis of the perturbation system (4.18) by showing how the divergent growth rate (3.3) may be recovered from it. The finite-angle Küppers–Lortz instability, as discussed in § 3, requires the B rolls to have the critical wavenumber and ignores the C rolls (because, when l and m are not small, these rolls are not nearly marginal). Thus to leading order $2km + l^2 = 0$, with the consequence that $|m| \ll |l|$ as $l \to 0$. If C is ignored (i.e. set to zero) and ω is regarded as slaved in the expression for $\dot{\omega}$ in (4.18), then $\omega = \tau\pi^2 A_0 B/4\varepsilon k^2 a^2 \sigma$ and it follows from the expression for $\dot{B}$ that $\lambda = \tau\pi^2\varepsilon^2 A_0^2/4lk\sigma a^2$ which is the divergent result (3.3) obtained earlier.

4.3. *The scaling of Ponty et al.*

In their analysis of the small-angle instability, Ponty *et al.* (1997) ignore the C rolls, but allow the vertical vorticity to evolve independently of the B rolls. The result is a truncation of (4.18) to the system

$$\lambda B = \varepsilon^3 l^{-1} k A_0 \omega, \tag{4.19}$$

$$\lambda\omega = \varepsilon^{-1}\beta_2 l^2 A_0 B - \sigma l^2 \omega, \tag{4.20}$$

where $m = O(l^2)$ and so does not appear in these equations at leading order. It follows that the growth rate λ satisfies the quadratic equation

$$\lambda^2 + \sigma l^2 \lambda - \frac{\tau\pi^2\varepsilon^2 A_0^2 l}{4ka^2} = 0. \tag{4.21}$$

This equation removes the blow-up of the growth rate at small angles between A rolls and perturbation rolls, and reduces to (3.3) if the term λ^2 is neglected, which corresponds to slaving ω to B. This is the equation from which Ponty *et al.* (1997) deduce the scaling $l = O(\varepsilon^{2/3})$ and $\lambda = O(\varepsilon^{4/3})$. However, this approximation, like the Küppers–Lortz result described above, is invalid for small l.

4.4. *Scaling 1: $l = O(\varepsilon^{2/5})$*

To determine the correct approach in the limit of small l, it is important first to consider the conditions under which the C mode can be ignored. We assume that B is

nearly marginal, so that $m = O(l^2)$ as $l \to 0$. Since the stability problem is linear, we lose no generality in choosing B to be $O(1)$, then the expression for $\dot{\omega}$ in (4.18) implies that $\omega = O(\varepsilon^{-1})$. This generates a forcing term in $\dot{C}$ of order ε^2/l, which may be balanced with the terms λC and $l^4 C$ if $C = O(\varepsilon^2/l^5)$ and $\lambda = O(l^4)$. Hence the result (3.3) is valid, and the C mode remains negligible, provided that $l \gg \varepsilon^{2/5}$. Furthermore, when this condition is satisfied, λ is no greater than $O(\varepsilon^{8/5})$. If $l = O(\varepsilon^{2/5})$ or smaller, C is of the same order as B and must be included in the analysis.

This motivates the following scaling:

$$B = O(1), \quad C = O(1), \quad \omega = O(\varepsilon^{-1}), \quad l = O(\varepsilon^{2/5}), \quad \lambda = O(\varepsilon^{8/5}). \tag{4.22}$$

In addition, the perturbation wavenumber $m = O(l^2)$, but we do not insist that $m = -l^2/2k$ (i.e. the wavenumber of the B rolls is not necessarily exactly critical). With this scaling, the system (4.18) simplifies to the leading-order equations

$$(\lambda + \gamma(mk + \tfrac{1}{2}l^2)^2)B - \frac{k\varepsilon^3 A_0 \omega}{l} = 0, \tag{4.23}$$

$$(\lambda + \gamma(-mk + \tfrac{1}{2}l^2)^2)C + \frac{k\varepsilon^3 A_0 \omega}{l} = 0, \tag{4.24}$$

$$\sigma\omega - \frac{\tau\pi^2 A_0 (B + C)}{4\varepsilon k^2 a^2} = 0, \tag{4.25}$$

from which it follows that λ satisfies the quadratic equation

$$\lambda^2 + 2\gamma(m^2k^2 + \tfrac{1}{4}l^4)\lambda + \gamma^2(m^2k^2 - \tfrac{1}{4}l^4)^2 + \frac{\tau\pi^2\varepsilon^2 A_0^2 \gamma m l}{2\sigma a^2} = 0. \tag{4.26}$$

As a consequence, if $m = 0$ the A rolls are stable to perturbations with this scaling.

However, for small l, the system is always unstable to modes with $\tau m l < 0$. If we assume (as we do throughout this paper) that $\tau > 0$ then in particular there is instability when the B rolls have critical wavelength (with $m = -l^2/2k$), corresponding to a rotation of the alignment of the axes of the rolls in the same sense as the rotation of the layer.

The scaling $l = O(\varepsilon^{2/5})$ is of particular significance because it is here that the growth rate achieves its maximum value. For perturbation rolls with the critical wavenumber, the positive root of (4.26) has the maximum value $\lambda_c = \gamma l_c^4/3$, where l_c satisfies

$$l_c^5 = \frac{9\tau\pi^2\varepsilon^2 A_0^2}{16\gamma k \sigma a^2}. \tag{4.27}$$

If the wavenumber of the perturbation rolls is not required to be critical, and the positive root of (4.26) is instead maximized over all values of l and m, we find $\lambda_{\max} = 5\gamma l_{\max}^4/12$ ($\approx 1.01\lambda_c$), where

$$l_{\max}^5 = \frac{\sqrt{3}\tau\pi^2\varepsilon^2 A_0^2}{4\gamma k \sigma a^2} \quad \text{and} \quad m_{\max} = \frac{2}{\sqrt{3}}\left(-\frac{l_{\max}^2}{2k}\right).$$

Since $2/\sqrt{3} > 1$, the fastest growing perturbation rolls have wavenumber slightly less than k_c.

It is instructive to examine the limits of large and small l, again with $m = -l^2/2k$. In the limit of large l the solution to (4.26) is $\lambda \sim \tau\pi^2\varepsilon^2 A_0^2/4lk\sigma a^2$, which matches

with (3.3). In the limit of small l, (4.26) gives

$$\lambda^2 \sim \frac{\tau\pi^2\varepsilon^2 A_0^2\gamma l^3}{4k\sigma a^2} \tag{4.28}$$

and so one might expect this expression to give the growth rate in the limit $l \to 0$. However, it then follows from (4.23) and (4.24) that $B + C$ is small, showing that a different scaling is required in order to capture this limit.

4.5. *Scaling 2:* $l = O(\varepsilon^{2/3})$

If $B + C$ is small and $B = O(1)$ then the expression for $\dot{\omega}$ in (4.18) implies that $\omega = O(\varepsilon^{-1}l)$ and that $B + C = O(l)$. Adding $\dot{B}$ to $\dot{C}$ then gives $l^4 = O(\varepsilon^2 l)$ and hence $l = O(\varepsilon^{2/3})$. The next scaling to be considered is therefore

$$B = O(1),\ C = O(1),\ B + C = O(l),\ \omega = O(\varepsilon^{-1/3}),\ l = O(\varepsilon^{2/3}),\ \lambda = O(\varepsilon^2), \tag{4.29}$$

with $m = O(l^2)$, so it follows that ω satisfies

$$\sigma\omega - \frac{\tau\pi^2 A_0(B + C)}{4\varepsilon k^2 a^2} + \frac{(\pi^4 - k^4)lA_0(B - C)}{4\varepsilon k^3 a^2} = 0. \tag{4.30}$$

The equations for B and C derived from (4.18) contain terms of mixed asymptotic orders, but a proper description of this scaling may be achieved from the corresponding leading-order equations for $B+C$ and $B-C$, which are each of consistent asymptotic order:

$$\lambda(B + C) = -2\varepsilon^2\alpha_3 A_0^2(B + C) - 6\varepsilon^3\alpha_6 A_0\omega - \alpha_2 ml^2(B - C)/k, \tag{4.31}$$

$$\lambda(B - C) = 2\varepsilon^3 k A_0\omega/l. \tag{4.32}$$

Hence a quadratic equation for λ is obtained:

$$\lambda^2 + \varepsilon^2 A_0^2\left(\frac{5(2k^2 - \pi^2)\pi^2\gamma}{48k^2\sigma^2} + \frac{\pi^2 - k^2}{2k^2\sigma} + \frac{\gamma k^2}{16}\right)\lambda + \frac{\tau\pi^2\gamma lm\varepsilon^2 A_0^2}{2\sigma a^2} + \frac{\varepsilon^4 A_0^4\gamma(\pi^2 - k^2)\zeta}{96k^4\sigma^3} = 0, \tag{4.33}$$

where

$$\zeta = 3\sigma^2 k^4 - 2\pi^2 k^2 + \pi^4$$

and $\zeta > 0$ for $\sigma > \sigma_c$. Note that with this scaling, the system can be stable or unstable, depending on the values of l and τ. In the limit $l \to \infty$, (4.33) simplifies to $\lambda^2 = -\tau\pi^2\varepsilon^2 A_0^2\gamma lm/2\sigma a^2$, which matches with the small-l solution of (4.26). For small l, (4.33) becomes

$$\lambda^2 + \varepsilon^2 A_0^2\left(\frac{5(2k^2 - \pi^2)\pi^2\gamma}{48k^2\sigma^2} + \frac{\pi^2 - k^2}{2k^2\sigma} + \frac{\gamma k^2}{16}\right)\lambda + \frac{\varepsilon^4 A_0^4\gamma(\pi^2 - k^2)\zeta}{96k^4\sigma^3} = 0. \tag{4.34}$$

which indicates that there is instability if $k > \pi$. Since k is determined by τ through (2.5), this condition for instability can be written as

$$\tau^2 > 4\pi^4 \approx 389.6.$$

4.6. *Scaling 3:* $l = O(\varepsilon)$

In each of the above scalings, the growth rate λ is small compared with l^2, so the ω mode is slaved to the B and C modes. We now seek a third and final scaling in which the vertical vorticity evolves independently:

$$B = O(1),\quad C = O(1),\quad B + C = O(l),\quad \omega = O(1),\quad l = O(\varepsilon),\quad \lambda = O(\varepsilon^2). \tag{4.35}$$

Again $m = O(l^2)$. With this scaling the following cubic for the growth rate λ is derived:

$$\lambda^3 + \left(\sigma l^2 + \frac{\varepsilon^2 A_0^2 \gamma \zeta}{48k^2\sigma^2}\right)\lambda^2 + \varepsilon^2 A_0^2 l^2 \left(\frac{5(2k^2-\pi^2)\pi^2\gamma}{48k^2\sigma} + \frac{\pi^2-k^2}{2k^2} + \frac{\gamma k^2\sigma}{16}\right)\lambda + \frac{\varepsilon^4 A_0^4 l^2 \gamma(\pi^2-k^2)\zeta}{96k^4\sigma^2} = 0. \quad (4.36)$$

Note that although we have eliminated τ from this equation using (2.5), the value of τ^2 determines k. It is significant that λ depends only on the squares of the quantities l and τ and is therefore independent of the direction of rotation; this point will be considered further in § 6.

In this scaling, the criterion for instability is again $\tau^2 > 4\pi^4$. This means that rotating convection rolls are unstable to rolls making an infinitesimal angle with the original rolls if the Taylor number is greater than $4\pi^4$. It is of interest to note that this result does not depend on the Prandtl number. Also, the critical value of the Taylor number is considerably lower than the value of 2285 obtained by Küppers & Lortz (1969) for instability to rolls at *finite* angles.

In the limit of large l, (4.36) matches with the small-l limit of (4.34). For small l, (4.36) has a negative eigenvalue independent of l and a pair of eigenvalues of order εl obeying

$$\lambda^2 \sim \tfrac{1}{2}\varepsilon^2 A_0^2 l^2 (k^2 - \pi^2). \quad (4.37)$$

The three scalings considered above, in which $l = O(\varepsilon^{2/5})$, $l = O(\varepsilon^{2/3})$ and $l = O(\varepsilon)$, were obtained from the system (4.18), which contains terms of different orders. We have therefore, for each scaling, confirmed our calculations by a more careful asymptotic analysis. The results are as stated above, and so we do not present the details.

5. The skew-varicose instability

A second significant mode of instability is the skew-varicose instability (Busse & Clever 1979*a*), which takes the form of a periodic modulation of the roll thickness in the axial direction. For non-rotating convection, rolls are skew-varicose unstable in a region given approximately by (Busse & Bolton 1984)

$$R - R_c > \tfrac{108}{7}\pi^2 k(k_c - k), \quad (5.1)$$

a result recovered by Bernoff (1994) by means of a self-consistent scaling in his amplitude equations. For rotating convection, we now apply a similar calculation to (4.16) and (4.17).

Stability is analyzed by considering rolls with $|\boldsymbol{k}| - k_c = O(\varepsilon^2)$ and perturbations with $|\boldsymbol{k}| - k_c = O(\varepsilon)$, in which case the growth rate λ of the instability is $O(\varepsilon^2)$. The instability is captured with rolls and perturbations of the form

$$A = \left[A_0 + \delta B(t)\exp \mathrm{i}(pX + qY) + \delta C^*(t)\exp -\mathrm{i}(pX + qY)\right]\exp \mathrm{i}\varepsilon K X,$$

$$\omega = \delta\omega(t)\exp \mathrm{i}(pX + qY) + \delta\omega^*(t)\exp -\mathrm{i}(pX + qY),$$

where $\delta \ll 1$, the essential terms in the amplitude equations being

$$A_t = \varepsilon^2\left(-\mathrm{i}kUA + \alpha_1 A + \alpha_2 A_{XX} - \alpha_3 A|A|^2\right) + \mathrm{i}\varepsilon^3\alpha_4 A_X,$$

$$\omega_t = \varepsilon\left[\beta_1(|A|^2)_{XY} + \beta_2((|A|^2)_{XX} - (|A|^2)_{YY})\right] + \sigma(\omega_{XX} + \omega_{YY})$$
$$+\mathrm{i}\varepsilon^2\left\{\beta_3\left[A(A^*_{YY} - 3A^*_{XX}) - \text{ c.c.}\right]_Y + \beta_4[AA^*_{XX} - \text{ c.c.}]_Y\right.$$
$$\left. + \beta_5[AA^*_{XX} - \text{ c.c.}]_X - 2\beta_5[AA^*_{XY} - \text{ c.c.}]_Y + \beta_6[AA^*_{YY} - \text{ c.c.}]_X\right\}.$$

In deriving an expression for λ, it is again convenient to consider the perturbation mode amplitudes in the combinations $B + C$ and $B - C$, so that the leading-order equations governing the growth rate are

$$\lambda(B + C) = -2\varepsilon^2\alpha_3 A_0^2(B + C) - \varepsilon^3 p(2\alpha_2 K + \alpha_4)(B - C),$$

$$\lambda(B - C) = \frac{2\varepsilon^2 kqA_0\omega}{p^2 + q^2} - \varepsilon^2\alpha_2 p^2(B - C),$$

$$\lambda\omega = \varepsilon[-\beta_1 pq + \beta_2(q^2 - p^2)]A_0(B + C) - \varepsilon^2\sigma(p^2 + q^2)\omega$$
$$-\varepsilon^2[q(q^2 - 3p^2)\beta_3 + p^2q\beta_4 + p^3\beta_5 - 2pq^2\beta_5 + pq^2\beta_6]A_0(B - C),$$

which are self-consistent if $\lambda = O(\varepsilon^2)$, $B - C = O(1)$, $\omega = O(1)$ and $B + C = O(\varepsilon)$.

The skew-varicose instability is most easily analyzed in the limit $p, q \to 0$, with $q = O(p)$. Then the appropriate scaling is $B - C = O(1)$, $\lambda = O(\varepsilon^2 p)$, $\omega = O(p^2)$ and $B + C = O(\varepsilon p)$, the dominant balance being

$$(B + C) = -\frac{\varepsilon p(2\alpha_2 K + \alpha_4)}{2\alpha_3 A_0^2}(B - C),$$

$$\lambda(B - C) = \frac{2\varepsilon^2 kqA_0\omega}{p^2 + q^2},$$

$$\lambda\omega = \varepsilon[-pq\beta_1 + (q^2 - p^2)\beta_2]A_0(B + C)$$
$$-\varepsilon^2[q(q^2 - 3p^2)\beta_3 + p^2q\beta_4 + p^3\beta_5 - 2q^2p\beta_5 + pq^2\beta_6]A_0(B - C).$$

It thus follows that

$$\lambda^2 = -\frac{2\varepsilon^4 kA_0^2 q}{p^2 + q^2}\left\{\frac{p(2\alpha_2 K + \alpha_4)}{2\alpha_3 A_0^2}\left[-pq\beta_1 + (q^2 - p^2)\beta_2\right]\right.$$
$$\left. + \left[q(q^2 - 3p^2)\beta_3 + p^2q\beta_4 + p^3\beta_5 - 2q^2p\beta_5 + pq^2\beta_6\right]\right\}, \quad (5.2)$$

with instability for $\lambda^2 > 0$.

In the non-rotating problem, the condition $\lambda^2 > 0$ for instability in (5.2) is precisely (5.1); see Bernoff (1994). In the rotating case, the analysis of (5.2) is more involved, but it easily seen that for small values of q/p,

$$\lambda^2 \sim 2\varepsilon^4 kA_0^2 pq\left\{\frac{\beta_2(2\alpha_2 K + \alpha_4)}{2\alpha_3 A_0^2} - \beta_5\right\}.$$

Rolls are therefore unstable to the skew-varicose instability regardless of their wavenumber (that is, regardless of the value of K), because the signs of p and q can be chosen to make $\lambda^2 > 0$. However, the growth rate of the skew-varicose instability is $O(\varepsilon^2)$ (and is asymptotically smaller than this in the limit of small p and q), so the small-angle instability described in § 4 grows more rapidly.

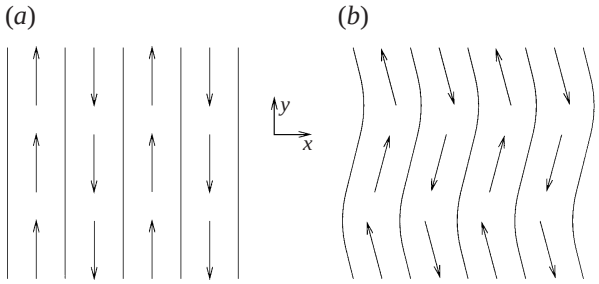

FIGURE 2. Plan view of convection rolls in the rapidly rotating limit. (*a*) The flow is predominantly along the rolls. (*b*) The flow is unstable to a mode in which the rolls become wavy.

6. The rapidly rotating limit and the physics of the small-angle instability

In the limit of rapid rotation, the equations for convection simplify considerably. The convection cells become narrow and the appropriate scaling is $\tau = O(k^3)$, $R_c = O(k^4)$. In this limit the solution to (2.5) is $k_c^6 \sim \tau^2\pi^2/2$. It follows that in the linear solution (2.8)–(2.11) the horizontal velocity component v_1 along the axis of the rolls is much greater than that across the rolls (figure 2*a*). Patterns of this type are referred to as 'anti-rolls' by Bosch Vivancos, Chossat & Melbourne (1995). Such patterns have the property that reflections in the plane act as -1, whereas in the usual case reflections act as $+1$. Thus in figure 2(*a*) the rolls have a symmetry of reflection in either x or y together with a reversal of the direction of flow (there is in fact no reflection symmetry in the line of the arrows; in this respect the figure is misleading). For rolls without rotation the reflection symmetry does not involve a reversal of the flow. Rapidly rotating convection therefore provides a physical example of a primary bifurcation to anti-rolls.

Interest in the rapidly rotating limit has recently arisen from the work of Bassom & Zhang (1994), who showed that the weakly nonlinear analysis can be extended into the fully nonlinear regime, so that nonlinear solutions with $R - R_c = O(R_c)$ can be obtained by solving a simple nonlinear eigenvalue problem.

In the rapidly rotating limit, rolls are unstable within each of the three scalings of §4 (because $\tau^2 \gg 4\pi^4$). It is therefore of interest to determine the dominant mode of instability in this case. For large k the appropriate scalings are

$$\tau = O(k^3),\ R_c = O(k^4),\ R_2 = O(k^4),\ A_0 = O(k),\ l = O(k),\ \gamma = O(k^{-2}). \tag{6.1}$$

In the scaling $l = O(\varepsilon^{2/5})$, the growth rate is given by (4.26). Substituting the scalings in (6.1) we find that the unstable eigenvalue is of order k. In the scalings $l = O(\varepsilon^{2/3})$ and $l = O(\varepsilon)$, governed by (4.33) and (4.36) however, the unstable eigenvalue is of order k^2. Hence it is these instabilities that dominate in the rapidly rotating limit.

It is important to note that the terms responsible for the instability in (4.33) and (4.36) are proportional to τ^2. This means that the instability is insensitive to the sign of τ. In the usual Küppers–Lortz instability, the sign of τ is important and rolls are unstable to perturbation rolls rotated in the same sense as τ. Thus we have found a new type of instability, which is driven by the rotation but does not depend on the direction of rotation.

We now consider the physical mechanism that drives this new instability. The instability derives from the nonlinear interaction of the original A rolls with the perturbation B and C rolls. In the linearized flow (2.8)–(2.11), τ appears only in

equation (2.10) for the flow v_1 along the rolls, so τ^2 terms must arise from the interaction of the flow along two sets of rolls, through the $\boldsymbol{u} \cdot \nabla \boldsymbol{u}$ term in (2.1). Such terms are then eliminated from our analysis using (2.5).

The instability also has the feature that $B + C$ is small. This means that the pattern of the perturbed rolls can be written via the planform function

$$h(x, y) \sim \varepsilon A_0 \sin kx + \delta B(\sin(kx + ly) - \sin(kx - ly)) \\ = \varepsilon A_0 \sin kx + 2\delta B \cos kx \sin ly. \quad (6.2)$$

These perturbed rolls have a wavy appearance, shown in figure 2(*b*). Instabilities of this type are referred to as the 'zig-zag' instability (Busse & Bolton 1984); these can occur in non-rotating convection if the original rolls have $k < k_c$. Here, however, the mechanism is quite different. A large-scale mean flow in the x-direction distorts the rolls into a wavy shape. The wavy rolls now advect momentum in such a way as to enhance the large-scale flow. Thus in figure 2(*b*), right-going fluid is carried to the upper half of the figure, while left-going fluid is carried to the lower half. This positive feedback allows the instability to grow. The mechanism is very similar to that responsible for the shearing instability of narrow convection rolls, described by Howard & Krishnamurti (1986) and Rucklidge & Matthews (1996).

Equivalently, the instability can be regarded simply as a hydrodynamic instability of the two-dimensional flow depicted in figure 2(*a*). This flow has inflection points of the right type to satisfy Rayleigh's criterion and Fjørtoft's theorem, so it may be unstable. The stability of the flow $v = \sin kx$, sometimes referred to as the Kolmogorov flow, was studied by Meshkalin & Sinai (1961), who showed that this flow becomes unstable as its Reynolds number increases, that the eigenvalue is real when the flow is unstable and that the first mode to become unstable as the Reynolds number is increased has a long wavelength.

7. Numerical simulations

In this section we describe numerical simulations of the instability of convection rolls in the presence of rotation. The motivation for this is two-fold. First, it is of interest to check the validity of the expressions obtained analytically for the growth rate of the instability. Secondly, numerical investigations reveal the nonlinear development of the instability. It is clear that the instability occurs through a pitchfork bifurcation, since a change of sign in the perturbation is equivalent to a shift of half a wavelength in the y-direction. However, it is important to determine whether the pitchfork is subcritical or supercritical. Although in principle this can be determined analytically, a numerical approach provides the answer more directly.

The numerical results were obtained using the convection code described by Cox & Matthews (1996). The method is pseudo-spectral, using Fourier modes in the horizontal directions and Chebyshev polynomials in the vertical direction. Periodic boundary conditions were applied in the horizontal directions. The numerical resolution used was $32 \times 32 \times 41$.

To investigate the growth rate of the instability four simulations were carried out, each at a different value of the Taylor number τ^2. The results are summarized in table 1. In each case the Prandtl number was 10 and the length of the box in the y-direction was 40, so the smallest admissible wavenumber in y is $l = 2\pi/40$. The length of the box in the x-direction was chosen so that five pairs of rolls with critical wavenumber were obtained. The initial condition used consisted of these five pairs

τ^2	k	R_c	R	λ(code)	λ(theory)
100	2.594	826	900	-0.13 ± 0.23i	-0.125 ± 0.23i
300	3.011	1075	1200	-0.13 ± 0.06i	-0.126 ± 0.059i
500	3.278	1275	1400	0.054	0.053
1000	3.710	1676	1800	0.130	0.129

TABLE 1. Comparison of numerical and analytical growth rates at different values of the Taylor number.

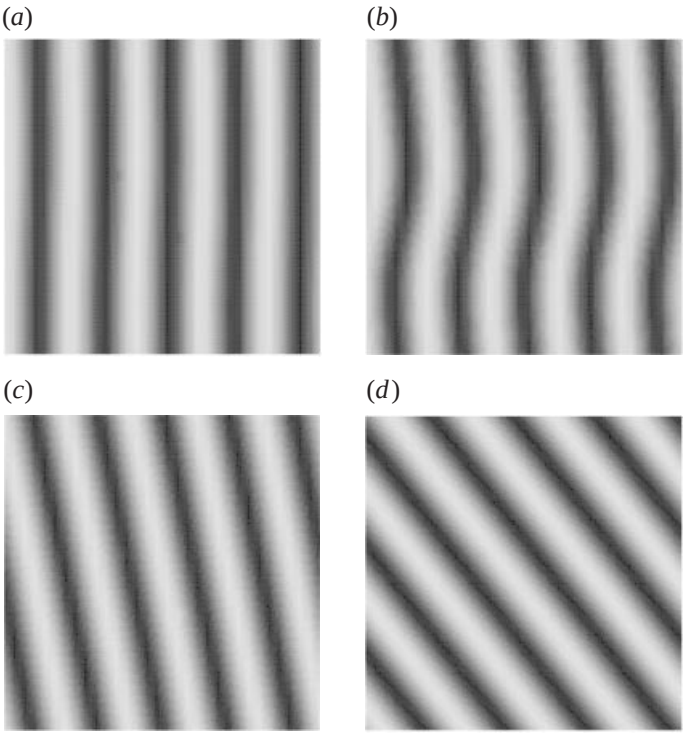

FIGURE 3. Evolution of the convection pattern with time. The plots show the vertical velocity, with dark shading for rising fluid and light shading for sinking fluid. (*a*) Aligned $(5,0)$ rolls ($t = 0$). (*b*) Wavy rolls ($t = 45$). (*c*) Re-aligned $(5,1)$ rolls ($t = 75$). (*d*) Re-aligned $(4,3)$ rolls ($t = 120$).

of rolls plus a small random perturbation, and the growth rate of the Fourier mode representing rolls with wave vector (k_c, l) was determined. Note that these rolls have $m = 0$, and do not lie on the circle of marginal modes. The theoretical results in the final column of table 1 were obtained from (4.36) and it is clear that the agreement between the numerical and theoretical growth rates is excellent.

To investigate the nonlinear development of the instability, one calculation was carried out at $\tau^2 = 500$ in a square box with sides of length $L = 9.584$ that contained five rolls with wavenumber k_c. The Prandtl number was 10 and the Rayleigh number was 1400 which is approximately $1.1R_c$. Again the initial condition used was five pairs of rolls with their axes aligned in the y-direction (figure 3*a*); these will be referred to as $(5,0)$ rolls, since their wave vector is $(5,0)2\pi/L$.

Since $\tau^2 > 4\pi^4$, these rolls are unstable. As shown in figure 4, the $(5,1)$ and $(5,-1)$ modes grow exponentially. In accordance with the predictions of § 4, the amplitudes

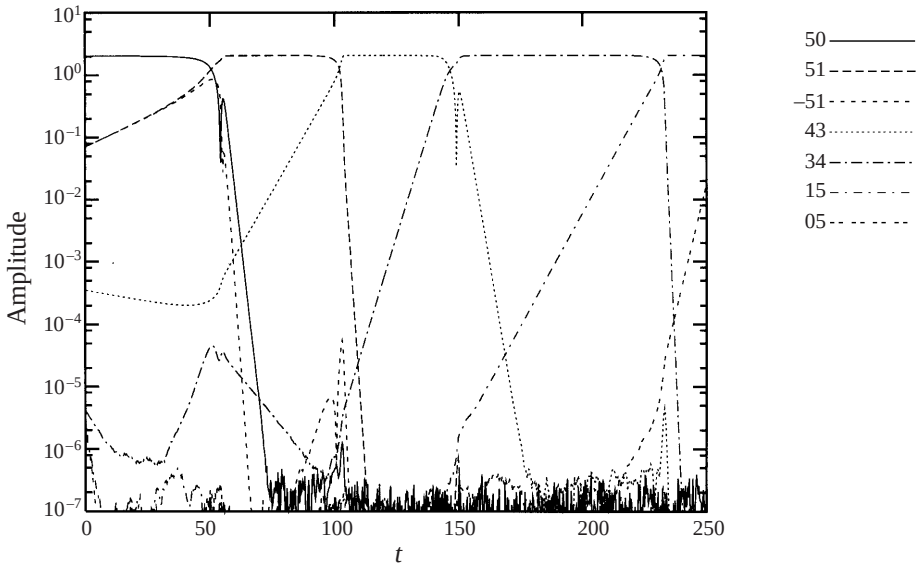

FIGURE 4. Nonlinear evolution of the instability of convection rolls, showing the logarithm of the amplitude of various modes as a function of time. The mode amplitude is half the maximum vertical velocity of the rolls, $\varepsilon A/2$.

of these two modes are almost identical, indicating that the instability is as shown in figure 2(*b*). This is confirmed by figure 3(*b*) which shows the pattern of convection at $t = 45$. If the instability were supercritical, the pattern would equilibrate at this stage, giving a stable pattern of wavy rolls. In fact however, the unstable modes continue to grow, indicating that the instability is subcritical. As the instability reaches its nonlinear phase, the $(5, 1)$ and $(5, -1)$ modes cease to be of equal amplitude and the $(5, 1)$ mode wins, leading to the pattern of $(5, 1)$ rolls shown in figure 3(*c*). These rolls are in turn unstable to the same instability, and are replaced by $(4, 3)$ rolls (figure 3*d*). The sequence then continues through $(3, 4)$ rolls, $(1, 5)$ rolls and $(0, 5)$ rolls (note that the $(3, 4)$ rolls have critical wavenumber, but the $(5, 1)$ rolls do not). Thus we find a structurally stable heteroclinic cycle connecting different roll solutions, all of which are unstable. This is analogous to the cycle found by Busse & Heikes (1980) for three sets of rolls at an angle of 60° that arises from the Küppers–Lortz instability at infinite Prandtl number. The exact number of modes in the cycle (ten in this case) depends on the size of the box chosen for the numerical simulation.

Structurally stable heteroclinic cycles, which exist in an open set of parameter values, are well known in dynamical systems theory (Armbruster, Guckenheimer & Holmes 1988) and in convection problems involving modal resonances (Jones & Proctor 1987; Proctor & Jones 1988). The behaviour of such heteroclinic cycles is dependent on machine precision. With infinite numerical precision, the cycle would become longer and longer as the solution gradually approached the infinite-period heteroclinic cycle. With finite precision (as here, where the computations were carried out with single precision arithmetic), numerical noise limits the time that can be spent near each fixed point of the heteroclinic cycle. This time is noise-dependent, and therefore slightly different results are obtained each time the computation is repeated.

8. Discussion

In this paper we have re-examined the Küppers–Lortz instability in the limit of small angles between the basic rolls and the perturbing rolls. In this limit, including only one perturbation roll leads to a divergent growth rate, indicating a failure of the asymptotic methods. To resolve this problem, two perturbation rolls and a mean flow must be considered. Three asymptotic regimes have been identified, in which the wavenumber l of the mean flow (or equivalently the angle between the perturbation rolls and the basic rolls) is of order ε, $\varepsilon^{2/3}$ and $\varepsilon^{2/5}$. The solutions for the growth rate of the instability match correctly across the different regimes. Those in the third regime dominate, and even exceed in magnitude the growth rates of the finite-angle Küppers–Lortz instability. The small-angle instability identified here also grows more rapidly than the skew-varicose instability.

For $l = O(\varepsilon)$, rolls are unstable if the Taylor number is greater than $4\pi^4$. This result is independent of the Prandtl number σ, although the growth rate of the instability does depend on σ and tends to zero for large σ. This new instability has a symmetry that is absent in the usual Küppers–Lortz instability, being independent of the direction of rotation. However, nonlinear effects lead to a preference for the roll alignment to rotate in the same sense as the rotation of the fluid layer. The instability is hydrodynamic in origin, driven by the flow along rolls which itself is driven by the Coriolis force. The mean flow leads to wavy rolls, and the waviness of rolls enhances the mean flow.

For $l = O(\varepsilon^{2/5})$, rolls are unstable for any value of the rotation rate, with a growth rate of order $\varepsilon^{8/5}$, smaller than the $\varepsilon^{4/3}$ predicted by Ponty *et al.* (1997), who did not include all the required modes. This instability does depend on the direction of rotation of the fluid layer.

One of the interesting consequences of this work concerns the case where the rotation vector is inclined. The first rolls to become unstable as R is increased are then those aligned with the horizontal component of the rotation vector, but these can be unstable. There is competition between the small-angle instability and the influence of the horizontal component of the rotation vector. Our preliminary numerical simulations show that rolls aligned at a small angle to the horizontal component of the rotation vector can be stable.

REFERENCES

Armbruster, D., Guckenheimer, J. & Holmes, P. 1988 Heteroclinic cycles and modulated travelling waves in systems with $O(2)$ symmetry. *Physica* **29D**, 257–282.

Barthelet, P. & Charru, F. 1998 Benjamin–Feir and Eckhaus instabilities with galilean invariance: the case of interfacial waves in viscous shear flows. *Eur. J. Mech.* B/*Fluids* **17**, 1–18.

Bassom, A. P. & Zhang, K. 1994 Strongly nonlinear convection cells in a rapidly rotating fluid layer. *Geophys. Astrophys. Fluid Dyn.* **76**, 223–238.

Bernoff, A. J. 1994 Finite amplitude convection between stress-free boundaries; Ginzburg–Landau equations and modulation theory. *Eur. J. Appl. Maths* **5**, 267–282.

Bosch Vivancos, I., Chossat, P. & Melbourne, I. 1995 New planforms in system of partial differential equations with Euclidean symmetry. *Arch. Rat. Mech. Anal.* **131**, 199–224.

Busse, F. H. & Bolton, E. W. 1984 Instabilities of convection rolls with stress-free boundaries near threshold. *J. Fluid Mech.* **146**, 115–125.

Busse, F. H. & Clever, R. M. 1979*a* Instabilities of convection rolls in a fluid of moderate Prandtl number. *J. Fluid Mech.* **91**, 319–335.

Busse, F. H. & Clever, R. M. 1979*b* Nonstationary convection in a rotating system. In *Recent Developments in Theoretical and Experimental Fluid Mechanics* (ed. U. Müller, K. G. Roesner & B. Schmidt), pp. 376–385, Springer.

Busse, F. H. & Heikes, K. E. 1980 Convection in a rotating layer: a simple case of turbulence. *Science* **208**, 173–175.

Chandrasekhar, S. 1961 *Hydrodynamic and Hydromagnetic Stability*. Oxford University Press.

Charru, F. & Barthelet, P. 1999 Secondary instabilities of interfacial waves due to coupling with a long-wave mode in two-layer Couette flow. *Physica* **125D**, 311–324.

Clever, R. M. & Busse, F. H. 1979 Nonlinear properties of convection rolls in a horizontal layer rotating about a vertical axis. *J. Fluid Mech.* **94**, 609–627.

Clune, T. & Knobloch, E. 1993 Pattern selection in rotating convection with experimental boundary conditions. *Phys. Rev.* E **47**, 2536–2550.

Cox, S. M. & Matthews, P. C. 1996 A pseudo-spectral code for convection with an analytical/numerical implementation of horizontal boundary conditions. *Intl J. Numer. Meth. Fluids* **25**, 151–166.

Cross, M. C., Daniels, P. G., Hohenberg, P. C. & Siggia, E. D. 1983 Phase-winding solutions in a finite container above the convective threshold. *J. Fluid Mech.* **127**, 155–183.

Howard, L. N. & Krishnamurti, R. 1986 Large-scale flow in turbulent convection: a mathematical model. *J. Fluid Mech.* **170**, 385–410.

Jones, C. A. & Proctor, M. R. E. 1987 Strong spatial resonance and travelling waves in Bénard convection. *Phys. Lett.* A **121**, 224–228.

Küppers, G. 1970 The stability of steady finite amplitude convection in a rotating plane layer. *Phys. Lett.* A **32**, 7–8.

Küppers, G. & Lortz, D. 1969 Transition from laminar convection to thermal turbulence in a rotating fluid layer. *J. Fluid Mech.* **35**, 609–620.

Meshkalin, L. D. & Sinai, Ia. G. 1961 Investigation of the stability of a stationary solution of a system of equations for the plane movement of an incompressible viscous liquid. *J. Appl. Math. Mech.* **25**, 1700–1705.

Newell, A. C. & Whitehead J. A. 1969 Finite bandwidth, finite amplitude convection. *J. Fluid Mech.* **38**, 279–303.

Ponty, Y., Passot, T. & Sulem, P. L. 1997 A new instability for finite Prandtl number rotating convection with free-slip boundary conditions. *Phys. Fluids* **9**, 67–75.

Proctor, M. R. E. & Jones, C. A. 1988 The interaction of two spatially resonant patterns in thermal convection. Part 1. Exact 1 : 2 resonance. *J. Fluid Mech.* **188**, 301–335.

Rucklidge, A. M. & Matthews, P. C. 1996 Analysis of the shearing instability in nonlinear convection and magnetoconvection. *Nonlinearity* **9**, 311–351.

Segel, L. A. 1969 Distant side-walls cause slow amplitude modulation of cellular convection. *J. Fluid Mech.* **38**, 203–224.

Soward, A. M. 1985 Bifurcation and stability of finite amplitude convection in a rotating layer. *Physica* **14D**, 227–241.

Swift, J. W. 1984 Convection in a rotating fluid layer. In *Contemporary Mathematics Volume 28 Fluids and Plasmas: Geometry and Dynamics* (ed. J. E. Marsden), pp. 435–448. American Mathematical Society.

Zippelius, A. & Siggia, E. D. 1983 Stability of finite-amplitude convection. *Phys. Fluids* **26**, 2905–2915.